Journal of Alloys and Compounds 500 (2010) 68–73

Contents lists available at ScienceDirect

Journal of Alloys and Compounds

journal homepage: www.elsevier.com/locate/jallcom

A rapid one-step mechanosynthesis and characterization of nanocrystalline $CaFe_2O_4$ with orthorhombic structure

L.J. Berchmans[a], M. Myndyk[b], K.L. Da Silva[b,c], A. Feldhoff[d], J. Šubrt[e], P. Heitjans[d], K.D. Becker[b], V. Šepelák[f,*,1]

[a] Electropyrometallurgy Division, Central Electrochemical Research Institute, Karaikudi 630006, Tamil Nadu, India
[b] Institute of Physical and Theoretical Chemistry, Braunschweig University of Technology, Hans-Sommer-Straße 10, 38106 Braunschweig, Germany
[c] Department of Physics, State University of Maringá, Maringá, Brazil
[d] Institute of Physical Chemistry and Electrochemistry, Leibniz University Hannover, Callinstraße 3-3A, 30167 Hannover, Germany
[e] Institute of Inorganic Chemistry, Academy of Sciences of the Czech Republic, 25068 Řež, Czech Republic
[f] Institute of Nanotechnology, Karlsruhe Institute of Technology, Herrmann-von-Helmholtz-Platz 1, 76344 Eggenstein-Leopoldshafen, Germany

ARTICLE INFO

Article history:
Received 22 February 2010
Received in revised form 15 March 2010
Accepted 17 March 2010
Available online 2 April 2010

Keywords:
Nanostructured materials
Mechanochemical processing
Microstructure
Core–shell morphology
Mössbauer spectroscopy
Transmission electron microscopy

ABSTRACT

$CaFe_2O_4$ nanopowders were prepared via single-step mechanochemical processing of two various mixtures of precursors: simple oxides (CaO and α-Fe_2O_3) and elemental metal and oxide powders (Ca and α-Fe_2O_3). The mechanically induced evolution of the CaO/α-Fe_2O_3 and Ca/α-Fe_2O_3 mixtures was followed by ^{57}Fe Mössbauer spectroscopy, XRD, and HR-TEM. The mechanosynthesis of $CaFe_2O_4$ proceeds very rapidly if starting from the metal/oxide system; after only 1 h of the mechanochemical treatment performed at room temperature, the synthesis of the complex oxide is almost completed. This is in a strong contrast to the conventional solid-state synthesis of $CaFe_2O_4$, which requires prolonged exposure (~20 h) at considerably elevated temperatures (~1400 K). It was revealed that mechanosynthesised $CaFe_2O_4$ nanoparticles with an average size of about 15 nm possess the core–shell structure consisting of an ordered inner core surrounded by a disordered surface shell with the thickness of about 1.9 nm. The main structural features of the surface shell of nanoparticles are distorted oxygen octahedra.

1. Introduction

The unique properties of nanocrystalline materials have kindled the interest on their newer and simpler preparative techniques [1]. Nanocrystalline materials behave indeed differently from their macroscopic counterparts; the enhanced properties of these materials are achieved from their large number of atoms residing in defect environments such as grain boundaries, near-surface layers, interfaces and triple junctions compared to coarse-grained polycrystalline materials [1–3].

Ferrite materials have opened a new vista in view of their technological applications such as high-density data storage [4], ferrofluid technology [5], magnetocaloric refrigeration [6], magnetically guided drug delivery [7], and heterogeneous catalysis [8,9]. The preparation of finely dispersed ferrites has been achieved by some novel methods like combustion synthesis [10], citrate gel process [11], and co-precipitation technique [12]. Nanosized ferrite materials have also been prepared by mechanical activation and mechanosynthesis, and their structural and magnetic properties have been elucidated [13–15].

The system Ca–Fe–O has for several decades been the subject of a great number of studies because of its applications as oxidation catalysts, high-temperature sensors, gas absorbers, etc. [16,17]. Nowadays, Ca–Fe–O complex oxides are promising materials for high-temperature electrochemical devices, such as ceramic membranes and electrodes for solid oxide fuel cells [18]. The phase diagram of CaO–Fe_2O_3 shows the existence of two compounds: $CaFe_2O_4$ with an orthorhombic structure and $Ca_2Fe_2O_5$ with the brownmillerite structure. $CaFe_2O_4$ is used as pigment [19] or as anode in lithium batteries [20] and as photocathodic material. $Ca_2Fe_2O_5$ is mostly employed as catalytic material [21].

Many methods have been employed to synthesise Ca–Fe–O complex oxides using simple oxides, carbonates, organic precursors, hydroxides, and also using solution chemistry. $CaFe_2O_4$, for example, has been synthesised using the ceramic method by annealing a mixture of $CaCO_3$/Fe_2O_3 for 24 h at 1453 K [20]. This demonstrates that the conventional solid-state synthesis of $CaFe_2O_4$ proceeds very slowly and requires prolonged exposure at considerably elevated temperatures. Also the Pechini process has been used to prepare crystalline $CaFe_2O_4$ at 1073 K [22], and

* Corresponding author. Tel.: +49 7247 828929; fax: +49 7427 826368.
E-mail address: vladimir.sepelak@kit.edu (V. Šepelák).
[1] On leave from the Slovak Academy of Sciences, Watsonova 45, 04353 Košice, Slovakia.

0925-8388/$ – see front matter © 2010 Elsevier B.V. All rights reserved.
doi:10.1016/j.jallcom.2010.03.199

the co-precipitation process has been successfully employed as well [23]. A novel synthesis procedure of both calcium ferrites ($CaFe_2O_4$ and $Ca_2Fe_2O_5$) was proposed in Ref. [24], starting from mechanically activated mixtures of organic precursors (calcium citrate tetrahydrate and iron(III) oxalate hexahydrate). It has been shown that the mechanically pre-activated mixtures yield, after 18 h annealing at 1073 K (or 1023 K), $Ca_2Fe_2O_5$ (or $CaFe_2O_4$). In comparison, the same compounds could be obtained, when starting from the non-activated mixtures, only by performing thermal treatments (for $t > 18$ h) at 1453 K ($Ca_2Fe_2O_5$) or 1373 K ($CaFe_2O_4$). Thus, mechanical pre-activation of the solid reactants considerably reduced the temperature and duration of the formation of the ferrite product during the subsequent step of thermal treatment. Moreover, $Ca_2Fe_2O_5$ has been prepared by subjecting to mechanical activation a mixture of $Ca(OH)_2/\alpha$-FeOOH and by heating the activated mixture between 673 and 1273 K [25]. The synthesis of $Ca_2Fe_2O_5$ has also been performed by thermal decomposition of $Ca[Fe(CN)_5NO]\cdot 4H_2O$ [26]. The above-given analysis of the literature procedures shows that various precursors have been employed for the synthesis of Ca-ferrites. It should be emphasized that the use of a metal/oxide precursor system has not been tested yet.

In this work, we report on the single-step synthesis of $CaFe_2O_4$ with the orthorhombic structure via high-energy milling of two various mixtures of precursors: simple oxides (CaO and α-Fe_2O_3) and elemental metal and oxide powders (Ca and α-Fe_2O_3). To the best of our knowledge, the single-step mechanosynthesis of nanosized $CaFe_2O_4$ particles has not been reported before. The present study clearly demonstrates that the yield of the mechanochemical reaction, leading to nanocrystalline $CaFe_2O_4$, is considerably higher if a Ca/α-Fe_2O_3 mixture is used rather than the CaO/α-Fe_2O_3 precursor system (at the same preparation conditions). The structure and morphology of the as-prepared nanocrystalline $CaFe_2O_4$ is characterized by ^{57}Fe Mössbauer spectroscopy, X-ray diffraction (XRD), and high-resolution transmission electron microscopy (HR-TEM).

2. Experimental

For the mechanochemical synthesis of $CaFe_2O_4$, stoichiometric mixtures of α-Fe_2O_3 and CaO as well as of α-Fe_2O_3 and granulated Ca metal (Merck, Darmstadt, Germany) were used as starting materials. The mixtures (5 g) were milled for various times (up to 12 h) in a Pulverisette 6 planetary ball mill (Fritsch, Idar-Oberstein, Germany) at room temperature. A grinding chamber (250 cm^3 in volume) and balls (10 mm in diameter) made of tungsten carbide were used. The ball-to-powder weight ratio was 40:1. Milling experiments were performed in air at 600 rpm.

Room temperature ^{57}Fe Mössbauer spectra were taken in transmission geometry using a ^{57}Co/Rh γ-ray source. The velocity scale was calibrated relative to ^{57}Fe in Rh. Recoil spectral analysis software [27] was used for the quantitative evaluation of the Mössbauer spectra. The degree of conversion of the mechanochemical reaction was calculated from the Mössbauer subspectral intensities.

The XRD patterns were collected using a PW1820 Philips powder diffractometer (Philips, Eindhoven, Netherlands) with Cu Kα radiation. The structure refinement was performed by Rietveld analysis of the XRD data using the Powder Cell program [28]. The JCPDS PDF database was utilized for the phase identification of the compounds [29]. The orthorhombic crystal structure of the mechanosynthesised $CaFe_2O_4$ was visualized using the Diamond program [30].

The morphology of powders and the sizes of individual crystallites were studied using a combined field-emission (scanning) transmission electron microscope (S)TEM (JOEL JEM-2100F) with an ultrahigh-resolution pole piece that provides a point resolution better than 0.19 nm at 200 kV. Prior to TEM investigations, powders were crushed in a mortar, dispersed in ethanol, and fixed on a copper-supported carbon grid.

3. Results and discussion

The mechanically induced evolution of the CaO/α-Fe_2O_3 and Ca/α-Fe_2O_3 mixtures submitted to high-energy milling was followed by ^{57}Fe Mössbauer spectroscopy (see Fig. 1). The spectra of both starting mixtures (CaO/α-Fe_2O_3 and Ca/α-Fe_2O_3) show a sextet with a magnetic hyperfine field of 51.6(4) T corresponding to α-Fe_2O_3. With increasing milling time, the sextet becomes asymmetric toward the inside of each line, slowly collapses, and is gradually replaced by a central doublet. This spectral component can be assigned to the $CaFe_2O_4$ product [17]; the detailed analysis of Mössbauer data is given below. In this context, it is interesting to note that the Mössbauer spectrum of α-Fe_2O_3 exhibits only a broadened sextet even if the particle size of the material reaches the nanoscale range; i.e., it does not display a superparamagnetic doublet and, thus, unreacted hematite can easily be detected in the Mössbauer spectra [3,13]. The fact that the spectral components, corresponding to educt (α-Fe_2O_3) and product ($CaFe_2O_4$) phases, are clearly resolved in the spectra, gives evidence that ^{57}Fe Mössbauer spectroscopy provides a very sensitive probe for the estimation of the yield of this mechanochemical reaction.

The decrease in the intensity of the Mössbauer sextet corresponding to α-Fe_2O_3, I_{sext}, relative to the total spectral intensity,

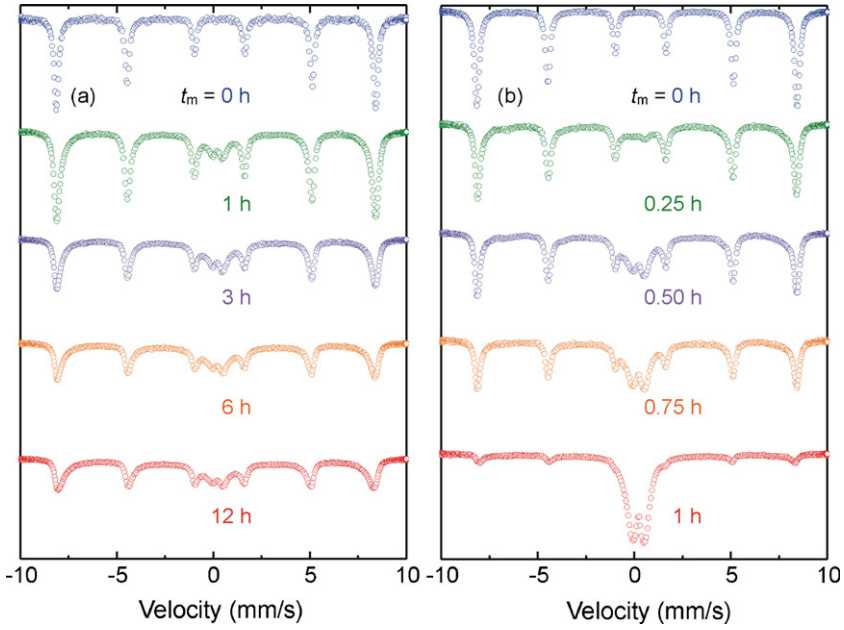

Fig. 1. Room temperature ^{57}Fe Mössbauer spectra of (a) the CaO/α-Fe_2O_3 mixtures and (b) the Ca/α-Fe_2O_3 powders milled for various times (t_m).

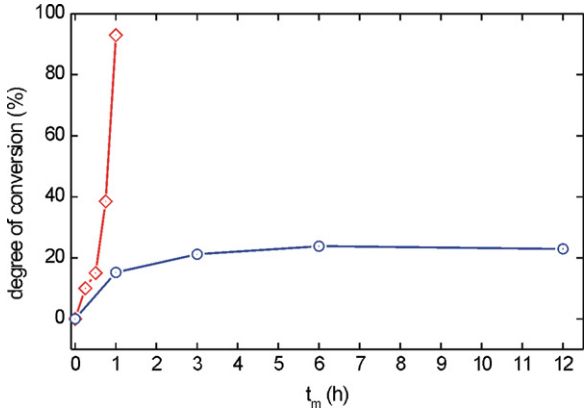

Fig. 2. Evolution of the degree of conversion of the mechanosynthesis of $CaFe_2O_4$ with milling time. Red and blue lines correspond to the mechanosynthesis starting from the $Ca/\alpha\text{-}Fe_2O_3$ and $CaO/\alpha\text{-}Fe_2O_3$ mixtures, respectively. The degree of conversion was calculated from the intensity of the Mössbauer sextet corresponding to $\alpha\text{-}Fe_2O_3$, I_{sext}, relative to the total spectral intensity, I_{tot}, according to $(1 - I_{sext}/I_{tot}) \times 100\%$. (For interpretation of the references to color in this figure legend, the reader is referred to the web version of this article.)

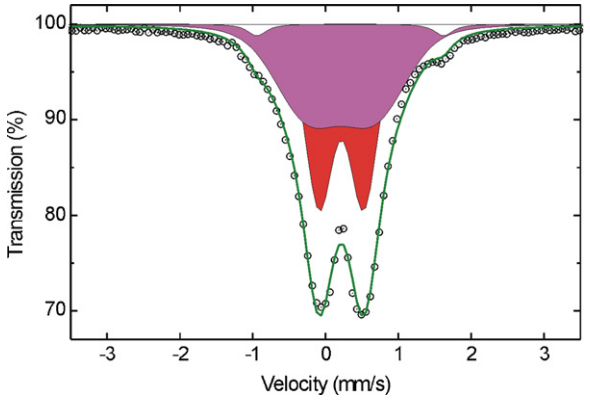

Fig. 3. The central part of the room temperature ^{57}Fe Mössbauer spectrum of mechanosynthesised $CaFe_2O_4$ prepared from the Ca/Fe_2O_3 mixture. Red and magenta subspectra correspond to Fe^{3+} cations in non-equivalent octahedral sites in the orthorhombic structure of the ferrite. The minor (~7%) white subspectrum is associated with Fe^{3+} ions in the unreacted $\alpha\text{-}Fe_2O_3$ phase. The Lorentzian width $\Gamma = 0.30$ mm/s resulted from the fit of the spectrum. (For interpretation of the references to color in this figure legend, the reader is referred to the web version of this article.)

I_{tot}, reflects a gradual conversion of the reactants to the ferrite phase during milling. As can be seen, the mechanosynthesis of $CaFe_2O_4$ from the metal/oxide system proceeds very rapidly; after only 1 h of the mechanochemical treatment, the synthesis of the complex oxide is almost completed – the degree of conversion of the mechanochemical reaction reaches about 93%. This is in strong contrast to the mechanochemical processing of the oxide/oxide precursor system; even after 12 h of the high-energy milling, the yield of the reaction reaches only about 23% (see Fig. 2).

The reason of the different behaviour of the metal/oxide and oxide/oxide precursor systems during the processing may lie in both the different chemical affinity and mechanical properties of Ca and CaO (the metal is more ductile than the oxide). Generally, the following factors are primarily responsible for a favourable effect of mechanochemical activation on the synthesis: dispersion and defect formation in starting reactants; the formation of fresh surfaces, which accelerates chemical interaction between reactants; and the mixing of components at a molecular level [31]. Although in the last years a surge of investigations in the field of mechanochemistry has resulted in the preparation of nanomaterials by forcing the system to acquire metastable and non-equilibrium configurations [2,15], it should be stated that the present mechanochemistry is mostly phenomenologically oriented, and the microscopic mechanisms of mechanochemical processes, including those of the mechanosynthesis of oxides, have scarcely been elucidated. In the present case, it is clear that oxygen is involved in the rapid one-step mechanosynthesis of $CaFe_2O_4$ if starting from the mixture of Ca metal and Fe_2O_3 ($Ca + Fe_2O_3 + (1/2)O_2 \rightarrow CaFe_2O_4$). This is in contrast to the solid–solid mechanochemical reaction between CaO and Fe_2O_3, which could directly lead to the ferrite ($CaO + Fe_2O_3 \rightarrow CaFe_2O_4$). Since the milling experiments were performed in air, it can be assumed that oxygen from the vial atmosphere plays an active role in the heterogeneous (solid–solid–gas) mechanochemical formation reaction. In the XRD patterns of the milled Ca/Fe_2O_3 mixture, it was observed that XRD peaks corresponding to Ca metal disappear within the initial stage of the milling process ($t_m \leq 0.5$ h), whereas the XRD lines belonging to Fe_2O_3 broaden gradually. Taking into account this observation, the following two scenarios can be assumed to occur at the reaction zone: (i) at first, the high-energy milling process decreases the particle size of Ca to the nanometer level, then, the mechanically activated Ca nanoparticles are oxidized by oxygen present in the vial atmosphere resulting in the formation of amorphous CaO (that cannot be detected by XRD), and finally, the reactive Ca^{2+} cations diffuse into the distorted rhombohedral structure of Fe_2O_3 and/or (ii) Ca atoms from nanocrystalline Ca metal are mechanically driven directly into the FeO_6 octahedron network of Fe_2O_3, followed by oxidation of a highly metastable $Ca\text{–}Fe_2O_3$ framework. Furthermore, it can be assumed that the mechanochemical transformation occurs at the moment of impact by the formation of high-energy localized sites of short lifetime (sometimes called "hot spots" or "thermal spikes" [32]). Impact-induced local heating and high pressures may provide further factors enhancing this synthesis mechanism of the complex oxide. To conclude, the identification of the factors representing the main driving force for mechanically induced formation processes, the elucidation of the microscopic mechanism(s), and the determination of rate-determining steps of mechanosynthesis represent major challenges for fundamental research and require further efforts.

In addition to the yield of the reaction, ^{57}Fe Mössbauer spectroscopy provided information on the charge states, the local symmetry and the magnetic state of iron ions in the mechanosynthesised $CaFe_2O_4$ material. The slightly asymmetrical central doublet in the spectrum of mechanosynthesised ferrite (see Fig. 3) indicates the presence of at least two crystallographically non-equivalent iron positions in the structure. This spectrum is hence fitted by using two quadrupole doublets corresponding to the ferrite and one sextet associated with the unreacted $\alpha\text{-}Fe_2O_3$ phase. The estimated isomer shifts values ($IS_1 = 0.216(7)$ mm/s, $IS_2 = 0.210(1)$ mm/s) of the doublet components are both typical for ferric (Fe^{3+}) ions in sites octahedrally coordinated by oxygen [33]. The quadrupole splittings of the spectral components ($QS_1 = 0.613(7)$ mm/s, $QS_2 = 0.924(2)$ mm/s) reflect different values of the electric field gradients acting on Fe^{3+} nuclei in the two non-equivalent octahedral positions of the mechanosynthesised material. These values are larger than those reported for the conventionally synthesised (bulk) $CaFe_2O_4$ ($QS_1 = 0.30$ mm/s, $QS_2 = 0.75$ mm/s) [18,34]. Note, however, that larger electric field gradients are typically observed for mechanosynthesised complex oxides [35]; they are produced by an asymmetric electronic charge distribution around the iron ions due to the distortion of polyhedra. It is found that for both octahedrally coordinated sites, the relative intensities of the spectral components are almost equal, reflecting the same occupation factor of iron cations within these structural units. Thus, the crystal chemical formula of the mechanosynthesised material can be written as $Ca[Fe]_{oct1}[Fe]_{oct2}O_4$, where

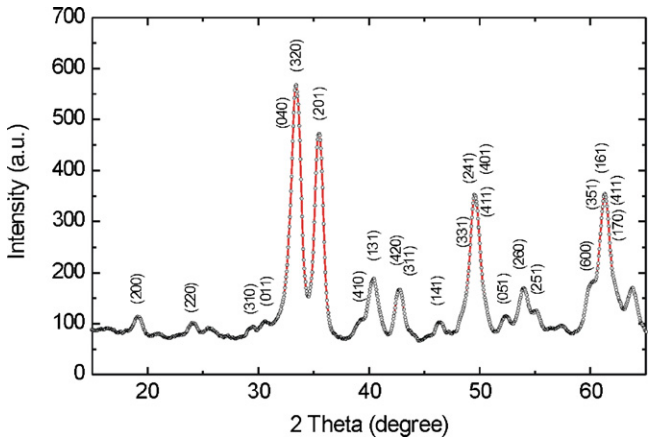

Fig. 4. XRD pattern of the mechanosynthesised complex oxide $CaFe_2O_4$. Diffraction lines of the mechanosynthesised product with orthorhombic structure (JCPDS PDF 32-0168) are denoted by Miller indices.

brackets enclose Fe^{3+} cations in non-equivalent distorted oxygen octahedra.

To determine the phase evolution of the Ca/α-Fe_2O_3 and CaO/α-Fe_2O_3 mixtures during high-energy milling by an independently supporting method, both mechanochemical routes to $CaFe_2O_4$ were also followed by XRD. Fig. 4 shows the XRD pattern of the mechanosynthesised $CaFe_2O_4$ product obtained after 1 h of milling of the Ca/α-Fe_2O_3 mixture. The Rietveld analysis of the XRD data of the mechanosynthesised material has revealed both an average crystallite size of about 18 nm and the presence of mean strains of 3×10^{-3} in the produced ferrite. Based on the analysis, the crystal structure of the mechanosynthesised product is found to be orthorhombic with the unit cell parameters $a = 9.214(3)$ Å, $b = 10.686(3)$ Å and $c = 3.004(4)$ Å. It should be noted that these unit cell parameters are smaller than those reported for bulk $CaFe_2O_4$, JCPDS PDF 32-0168 ($a = 9.230$ Å, $b = 10.705$ Å, $c = 3.024$ Å) [29]. The interatomic distances in $[FeO_6]_{oct1}$ and $[FeO_6]_{oct2}$ octahedra of the mechanosynthesised ferrite are found to be different from those of the bulk material (see Table 1). This finding explains the different QS values, determined by ^{57}Fe Mössbauer spectroscopy, for nanocrystalline and bulk $CaFe_2O_4$. Thus, the relatively large QS values, i.e., large electric field gradients, for mechanosynthesised $CaFe_2O_4$ ($QS_1 = 0.613(7)$ mm/s, $QS_2 = 0.924(2)$ mm/s) are caused by a highly-asymmetric charge distribution around Fe nuclei originating from the different bond lengths in $[FeO_6]_{oct1}$ and $[FeO_6]_{oct2}$ octahedra. Consequently, the smaller QS values for bulk $CaFe_2O_4$ ($QS_1 = 0.30$ mm/s, $QS_2 = 0.75$ mm/s) reflect the presence of distorted but more symmetric FeO_6 octahedra in its structure, i.e., octahedra with more converging Fe–O bond lengths. The appearance of highly-distorted $[FeO_6]_{oct1}$ and $[FeO_6]_{oct2}$ octahedra in the structure of mechanosynthesised $CaFe_2O_4$ can be a consequence of the above-mentioned scenarios of microscopic mechanisms of the mechanosynthesis, at which the relatively large Ca species are mechanically driven into the FeO_6 octahedron network. Based on the crystallographic data obtained by Rietveld analysis, the structure of the mechanosynthesised $CaFe_2O_4$ is illustrated in Fig. 5. As seen, the structure with two distinct iron sites is composed by corner- and edge-shared FeO_6 octahedra, which form pseudo-triangular tunnels where eightfold-coordinated Ca^{2+} cations are located.

Table 1
The interatomic distances in $[FeO_6]_{oct1}$ and $[FeO_6]_{oct2}$ octahedra derived from the Rietveld analysis of the XRD data of nanocrystalline mechanosynthesised $CaFe_2O_4$ in comparison with the bond lengths reported for bulk $CaFe_2O_4$ [29].

Length of Fe–O bond [Å]			
Nanocrystalline $CaFe_2O_4$		Bulk $CaFe_2O_4$	
$[FeO_6]_{oct1}$	$[FeO_6]_{oct2}$	$[FeO_6]_{oct1}$	$[FeO_6]_{oct2}$
1.973(1)	1.952(2)	1.9953	1.9797
2.003(2)	1.952(2)	2.0321	1.9797
2.047(4)	1.990(5)	2.0699	2.0168
2.047(4)	2.026(6)	2.0699	2.0404
2.097(3)	2.097(5)	2.0712	2.0874
2.097(3)	2.097(5)	2.0712	2.0874

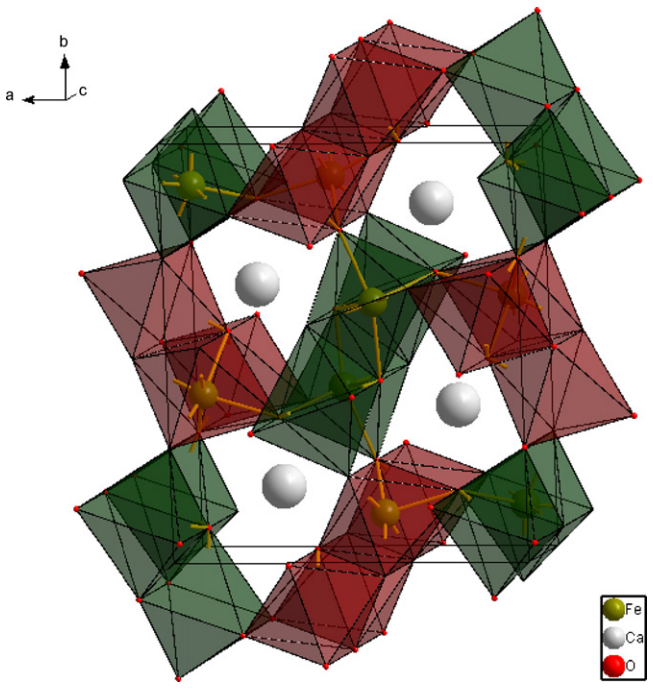

Fig. 5. The crystal structure of $CaFe_2O_4$.

Representative TEM micrographs of nanocrystalline mechanosynthesised $CaFe_2O_4$ at high magnification are shown in Fig. 6. HR-TEM reveals the presence of nanoparticles of irregular shape with a relatively broad size distribution ranging from about 8 nm to 30 nm (see Fig. 6a), resulting in the average particle size of about 15 nm. As seen, the mechanosynthesised $CaFe_2O_4$ nanoparticles possess the core–shell structure consisting of an ordered inner core surrounded by a disordered surface shell region. The thickness of the surface shell was found to be about 1.9 nm, Fig. 6b. The high-resolution TEM images show lattice fringes corresponding to the crystallographic plane (220) ($d = 3.5$ Å) of the $CaFe_2O_4$ phase. The lattice fringes cross the whole particle core demonstrating its single-crystalline character.

Assuming a spherical shape of mechanosynthesised $CaFe_2O_4$ nanoparticles with $D = 15$ nm and $t = 1.9$ nm, the volume fraction of surface shell regions was calculated to be $w = 0.584$. This indicates that about 58% of atoms in the mechanosynthesised ferrite are in a structurally disordered state located in the surface shell of the nanoparticles. It can be assumed that distorted octahedra, evidenced by Mössbauer spectroscopy and XRD, are located in the surface shell of nanoparticles. The structurally non-uniform core–shell structure of nanoparticles with the relatively large volume fraction of surface shell regions (~50%) has recently been reported for mechanosynthesised $MgFe_2O_4$ [3], $NiFe_2O_4$ [13], $LiNbO_3$ [36], and Ca_2SnO_4 [37]. The shell thickness in mechanosynthesised $CaFe_2O_4$ is comparable to that observed in other nanosized complex oxides prepared by mechanochemical routes [3,13,36–38].

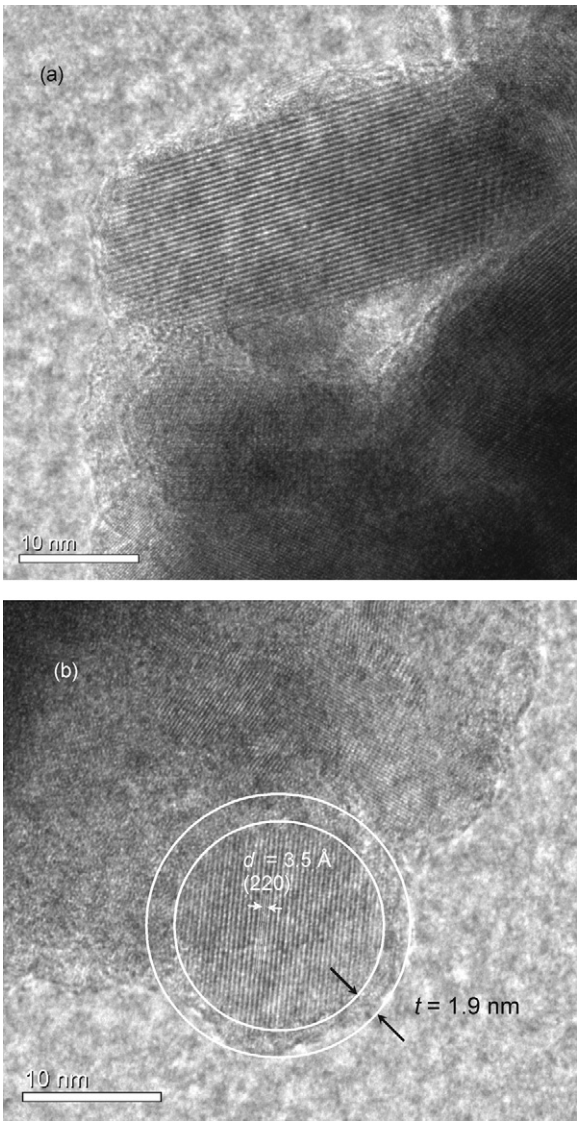

Fig. 6. (a) High-resolution TEM image demonstrating the presence of $CaFe_2O_4$ nanoparticles of irregular shape with a relatively broad size distribution ranging from about 8 nm to 30 nm. (b) The core–shell configuration of mechanosynthesised nanoparticles with the thickness of the surface shell of about 1.9 nm is evident. The lattice fringes correspond to the crystallographic plane (220) (d = 3.5 Å) of the $CaFe_2O_4$ phase (JCPDS PDF 32-0168).

4. Conclusions

The possibility of preparing calcium ferrite through chemical transformation by mechanical energy (mechanosynthesis) has been studied using both Ca/α-Fe_2O_3 and CaO/α-Fe_2O_3 mixtures as the reactants. Nanosized $CaFe_2O_4$ with an average crystallite size of about 15 nm has been synthesised in 1 h via one-step mechanochemical route from the mixture of Ca and α-Fe_2O_3 precursors at room temperature. Compared to the conventional solid-state chemical route, the process used here represents a simple, high-yield, lower temperature, and faster procedure for the synthesis of $CaFe_2O_4$ nanocrystals. It is evidenced that the Mössbauer active ^{57}Fe nuclei provide a very sensitive probe for the accurate determination of the degree of conversion of the mechanochemical reaction. From the XRD data, the crystal structure of the mechanosynthesised $CaFe_2O_4$ product is found to be orthorhombic. Due to the ability of ^{57}Fe Mössbauer spectroscopy to discriminate between probe nuclei on inequivalent crystallographic sites, valuable insight into the local structural disorder in mechanosynthesised $CaFe_2O_4$ is obtained. Based on the results of ^{57}Fe Mössbauer and XRD analyses, the crystal chemical formula of the mechanosynthesised material can be written as $Ca[Fe]_{oct1}[Fe]_{oct2}O_4$, where brackets enclose Fe^{3+} cations in non-equivalent distorted oxygen octahedra. High-resolution TEM studies have revealed that the mechanosynthesised $CaFe_2O_4$ nanoparticles possess a non-uniform configuration consisting of an ordered core with orthorhombic structure surrounded by a disordered surface shell region. The observed lattice fringes crossing the whole particle core demonstrate the single-crystalline character of the ferrite nanoparticles. The thickness of the disordered surface shell is found to be about 1.9 nm. The volume fraction of surfaces shell regions in the mechanosynthesised nanomaterial is estimated to be about 58%. It can be assumed that the distorted FeO_6 octahedra are located in the near-surface regions of nanoparticles.

Acknowledgements

The present work was supported by the German Research Foundation (DFG) in the framework of the Priority Programme *"Crystalline Non-equilibrium Phases"* (SPP 1415). The authors (L.J.B., K.D.B., V.Š.) thank the German Academic Exchange Service (DAAD) and the Department of Science and Technology (DST), Government of India, for supporting their mutual research stays at the Braunschweig University of Technology, the Karlsruhe Institute of Technology, and the Central Electrochemical Research Institute, Karaikudi, within a German-Indian (DAAD-DST) Joint Research Collaboration Programme. Partial support by the APVV (0728-07), the VEGA (2/0065/08), and the Academy of Sciences of the Czech Republic is gratefully acknowledged.

References

[1] B. Kubias, M.J.G. Fait, R. Schlögl, Mechanochemical methods, in: G. Ertl, H. Knözinger, F. Schüth, J. Weitkamp (Eds.), Handbook of Heterogeneous Catalysis, Wiley-VCH, Weinheim, 2008, pp. 571–583.
[2] F. Delogu, G. Mulas, Experimental and Theoretical Studies in Modern Mechanochemistry, Transworld Research Network, Kerala, 2010.
[3] V. Šepelák, A. Feldhoff, P. Heitjans, F. Krumeich, D. Menzel, F.J. Litterst, I. Bergmann, K.D. Becker, Chem. Mater. 18 (2006) 3057–3067.
[4] M.H. Kryder, E.C. Gage, T.W. Mcdaniel, W.A. Challener, R.E. Rottmayer, G.P. Ju, Y.T. Hsia, M.F. Erden, Proc. IEEE 96 (2008) 1810–1835.
[5] C. Holm, J.J. Weis, Curr. Opin. Colloid Interfac. Sci. 10 (2005) 133–140.
[6] B.G. Shen, J.R. Sun, F.X. Hu, H.W. Zhang, Z.H. Cheng, Adv. Mater. 21 (2009) 4545–4564.
[7] P. Tartaj, Curr. Nanosci. 2 (2006) 43–53.
[8] R.A. Buyanov, V.V. Molchanov, V.V. Boldyrev, Catal. Today 144 (2009) 212–218.
[9] C.A. Martinez-Huitle, E. Brillas, Appl. Catal. B 87 (2009) 105–145.
[10] R.K. Selvan, C.O. Augustin, V. Šepelák, L.J. Berchmans, C. Sanjeeviraja, A. Gedanken, Mater. Chem. Phys. 112 (2008) 373–380.
[11] C.O. Augustin, R.K. Selvan, R. Nagaraj, L.J. Berchmans, Mater. Chem. Phys. 89 (2005) 406–411.
[12] L.J. Berchmans, R. Sindhu, S. Angappan, C.O. Augustin, J. Mater. Process. Technol. 207 (2008) 301–306.
[13] V. Šepelák, I. Bergmann, A. Feldhoff, P. Heitjans, F. Krumeich, D. Menzel, F.J. Litterst, S.J. Campbell, K.D. Becker, J. Phys. Chem. C 111 (2007) 5026–5033.
[14] M.J.N. Isfahani, M. Myndyk, V. Šepelák, J. Amighian, J. Alloy. Compd. 470 (2009) 434–437.
[15] V.V. Boldyrev, Russ. Chem. Rev. 75 (2006) 177–189.
[16] N.-O. Ikenaga, Y. Ohgaito, T. Suzuki, Energy Fuels 19 (2005) 170–179.
[17] D. Hirabayashi, Y. Sakai, T. Yoshikawa, K. Mochizuki, Y. Kojima, K. Suzuki, K. Ohshita, Y. Watanabe, Hyperfine Interact. 167 (2006) 809–813.
[18] E.V. Tsipis, Y.V. Pivak, J.C. Waerenborgh, V.A. Kolotygin, A.P. Viskup, V.V. Kharton, Solid State Ionics 178 (2007) 1428–1436.
[19] S.B. Hana, F.F. Abdel-Mohsen, H.S. Emira, Interceram. 54 (2005) 106–110.
[20] N. Sharma, K.M. Shaju, G.V. Subba Rao, B.V.R. Chowdari, J. Power Sources 124 (2003) 204–212.
[21] D. Hirabayashi, T. Yoshikawa, K. Mochizuki, K. Suzuki, Y. Sakai, Catal. Lett. 110 (2006) 269–274.
[22] R.A. Candeia, M.I.B. Bernardi, E. Longo, I.M.G. Santos, A.G. Souza, Mater. Lett. 58 (2004) 569–572.
[23] X. Ma, M. Zheng, W. Liu, Y. Qian, B. Zhang, W. Liu, J. Hazard. Mater. 127 (2005) 156–162.

[24] V. Berbenni, A. Marini, G. Bruni, C. Milanese, J. Anal. Appl. Pyrol. 82 (2008) 255–259.
[25] L.A. Isupova, S.V. Tsibulya, G.N. Kryukova, A.A. Budneva, E.A. Paukshtis, G.S. Litvak, V.P. Ivanov, V.N. Kolomiichuk, Yu.T. Pavlyukhin, V.A. Sadykov, Kinet. Catal. 43 (2002) 122–129.
[26] M.I. Gómez, J.A. de Morán, R.E. Carbonio, P.J. Aymonino, J. Solid State Chem. 142 (1999) 138–145.
[27] K. Lagarec, D.G. Rancourt, Recoil – Mössbauer Spectral Analysis Software for Windows, University of Ottawa, Ottawa, ON, 1998.
[28] W. Kraus, G. Nolze, PowderCell for Windows, Federal Institute for Materials Research and Testing, Berlin, Germany, 2000.
[29] Joint Committee on Powder Diffraction Standards (JCPDS) Powder Diffraction File (PDF), International Centre for Diffraction Data, Newton Square, PA, 2004.
[30] Diamond – Crystal and Molecular Structure Visualization Software, Crystal Impact GbR, Bonn, Germany.
[31] E.G. Avvakumov, Mechanical Methods of Activating Chemical Processes, Nauka, Novosibirsk, 1986 (in Russian).
[32] V. Šepelák, M. Menzel, K.D. Becker, F. Krumeich, J. Phys. Chem. B 106 (2002) 6672–6678.
[33] F. Menil, J. Phys. Chem. Solids 46 (1985) 763–789.
[34] A. Hudson, H.J. Whitfield, J. Chem. Soc. A (1967) 376–378.
[35] V. Šepelák, K.D. Becker, J. Mater. Synth. Proces. 8 (2000) 155–166.
[36] P. Heitjans, M. Masoud, A. Feldhoff, M. Wilkening, Faraday Discuss. 134 (2007) 67–82.
[37] V. Šepelák, K.D. Becker, I. Bergmann, S. Suzuki, S. Indris, A. Feldhoff, P. Heitjans, C.P. Grey, Chem. Mater. 21 (2009) 2518–2524.
[38] M. Muroi, R. Street, P.G. McCormick, J. Amighian, Phys. Rev. B 63 (2001), 184414-1–7.